JACS
JOURNAL OF THE AMERICAN CHEMICAL SOCIETY
pubs.acs.org/JACS
Article

Single Ensemble Non-exponential Photoluminescent Population Decays from a Broadband White-Light-Emitting Perovskite

Joseph E. Thomaz, Kurt P. Lindquist, Hemamala I. Karunadasa,* and Michael D. Fayer*

Cite This: J. Am. Chem. Soc. 2020, 142, 16622−16631
Read Online

ABSTRACT: The mechanism of white-light emission from layered Pb-X (X = Cl or Br) perovskites following UV excitation has generated considerable interest. Prior time-dependent studies indicated that the broadband photoluminescence (PL) from (110) perovskites arises from a distribution of self-trapped excitonic sites emitting in different regions of the visible spectrum with different decay dynamics. Here, using time-correlated single photon counting to study single crystals, we show that the white-light emission decay from the (110) perovskite (EDBE)$PbBr_4$ (EDBE = 2,2′-(ethylenedioxy)bis(ethylammonium)) behaves as a single ensemble. Following the rapid decay (0.6 ns) of a small spectral side band, the broad emission line shape is constant to 100 ns. We propose that rapid local structural fluctuations cause the self-trapped excitons (STEs) to experience a wide range of energies, resulting in the very broad PL. The STEs sample fluctuating local environments on time scales fast compared to the PL, which averages the PL decay at all emission wavelengths, yielding single ensemble PL dynamics. Although emission occurs from a very wide, inhomogeneously broadened spectral line with time-averaged single ensemble luminescence dynamics, the decay is tri-exponential. Two heuristic models for the tri-exponential decay involving defects are discussed. Spin-coated films show faster non-exponential decays with the slowest component of the crystal PL absent. Like the crystals, the film PL decays as a single ensemble. These results demonstrate that the broadband emission decay of (EDBE)$PbBr_4$ arises from a time-averaged single ensemble and not from a set of excited states emitting with distinct luminescence decays at different wavelengths.

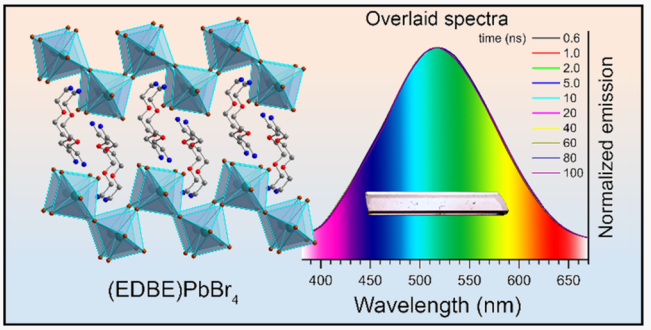

1. INTRODUCTION

Although initially discovered in 1839, perovskites, a broad family of crystalline materials, have seen a great reemergence in recent times. In particular, halide-perovskite semiconductors show promise in a wide variety of fields, most notably as photovoltaic absorbers and as illumination sources.[1] Several experiments have been performed, in both the ground and excited states, to inspect the lattice dynamics of halide perovskites.[2−5] It is believed that the flexible nature of the halide-perovskite lattice is at least partially responsible for their interesting properties. The most-studied halide perovskites may be divided into two categories: three-dimensional (3D) and two-dimensional (2D; also known as layered perovskites). The 3D halide perovskites have chemical formulas of the form A^IBX_3 (X = I, Br, or Cl), whereas in 2D halide perovskites the formula is $A^I{}_2BX_4$ (or equivalently $A^{II}BX_4$).[6] In cases where the A-site organic cation is too large to fit into a 3D lattice, one can generate a hybrid organic−inorganic 2D perovskite.[6]

The 2D halide perovskites are being investigated as phosphors,[7] including as broadband white-light emitters. The high binding energy and large oscillator strength of excitons (excited electron−hole pairs) in 2D perovskites typically result in strong, narrowband photoluminescence (PL), even at room temperature.[8,9] These exciton binding energies are much higher than those seen in their 3D counterparts because of the spatial and dielectric confinement of the inorganic layers.[10] However, a small subset of 2D perovskites exhibit highly Stokes shifted broadband PL at room temperature, with near-ultraviolet photoexcitation resulting in broad visible emission; in some perovskites, the emission is sufficiently broad to cover the entire visible spectrum, resulting in "white light".[11] This intrinsic white-light emission makes 2D perovskites promising candidates for use as illumination sources. Broadband white-light emission from the inorganic layers of 2D perovskites was discovered by Karunadasa and co-workers in 2014. These 2D lead-halide perovskites were (EDBE)PbX_4 (X = Cl or Br; Figure 1) and (*N*-MEDA)PbX_4 (X = Br), where EDBE is 2,2′-(ethylenedioxy)bis(ethylammonium), and *N*-MEDA is N^1-methylethane-1,2-diammonium.[9,12] By 2018, nine room-

Received: May 23, 2020
Published: September 10, 2020

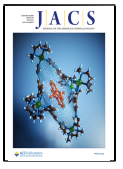

https://dx.doi.org/10.1021/jacs.0c05636
J. Am. Chem. Soc. 2020, 142, 16622−16631

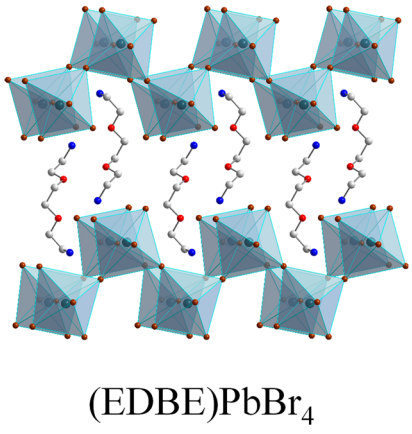

Figure 1. Crystal structure of the broadband white-light-emitting 2D perovskite (EDBE)$PbBr_4$ (EDBE = 2,2′-(ethylenedioxy)bis(ethylammonium)). Turquoise, brown, red, blue, and gray spheres represent Pb, Br, O, N, and C atoms, respectively. H atoms are omitted for clarity. The unit cell volume is 1592.47 $Å^3$, where the cell dimensions are a = 6.15 Å, b = 28.74 Å, and c = 9.02 Å, with the b axis perpendicular to the 2D sheets.

temperature broadband white-light-emitting perovskites had been observed, and this number continues to increase.[9,11,13−18]

One of the most desirable aspects of artificial indoor illumination is its ability to accurately reproduce the color of objects relative to how they appear in natural light. A quantitative measure of this is known as the color rendering index (CRI), with values ranging from 0 to 100, where 100 is standardized daylight.[19] To date, the incandescent light bulb remains one of the highest-quality light sources, with a CRI value of 98; however, its poor energy efficiency and lifespan make it less than ideal as an illumination source.[20] Light-emitting diodes (LEDs) offer poorer CRI values, but they can be improved by mixing multiple LEDs and phosphor coatings to give values between 60 and 95. LEDs offer much a higher energy efficiency and lifespan in comparison to incandescent bulbs.[21] Many of the white-light-emitting perovskites have CRI values above 80 for a single emitter, comparable to mixed arrays of LEDs and suggesting their potential for lighting applications.[11] Indeed, it is unusual for a single emitter to span the entire visible spectrum. Thus, the source of the broadband emission from 2D perovskites has been studied since 2014.

We attributed the exceptionally broad emission of (110) Pb-Br perovskites to intrinsic and extrinsic exciton self-trapping.[9,12,22] In intrinsic self-trapping, strong exciton−lattice coupling causes large structural distortions in the excited state. This lattice deformation leads to a homogeneously broadened emission width, while both the lattice distortion and the stabilization of the self-trapped exciton with respect to the free exciton results in the large Stokes shift (Figure 2A). Homogeneous broadening by itself is unlikely to generate enough spectral width to be responsible for the white-light emission. Self-trapping events that occur near native lattice defects (e.g., lattice vacancies), also called extrinsic self-trapping, can cause inhomogeneities in the excited state, resulting in a distribution of self-trapped states.[22] Emission from such distinct environments can give rise to different optical frequencies and lifetimes, further increasing the emission width (Figure 2B). Previously, extrinsic self-trapping was invoked, in addition to intrinsic self-trapping, to explain the wavelength dependence of the broad emission lifetime seen in pressed pellets of the (110) perovskite (*N*-MEDA)$PbBr_4$.[22] A similar study on (EDBE)$PbBr_4$ also showed different PL decay dynamics in the broad emission as a function of wavelength, attributed to different emissive species.[23]

Various spectroscopies have been used to study the photoluminescent emission in halide perovskites,[24−27] which can contribute to a fundamental understanding of the white-light-emission mechanism. Here, we expand the study of the emission mechanism in (110) perovskites by studying (EDBE)$PbBr_4$ (Figure 1), which has one of the highest photoluminescent quantum efficiencies (PLQE ≈ 9%) and CRI values (84) for a white-light-emitting perovskite, to further understand the origins of the broad bandwidth emission. By collecting a large number of spectra over a wide range of times, from 0.2 to 100 ns, and eliminating the role of grain boundaries and surfaces through the study of single crystals, we find that the broad emission decay (after the decay of a small distinct side peak in ∼600 ps) is wavelength independent, i.e., all energies of the broad emission have identical decay dynamics. Intriguingly, despite displaying single ensemble decay dynamics, the emissions from both crystals and films are non-exponential. Two heuristic models, involving defects, are discussed as possible explanations for the non-exponential behavior.

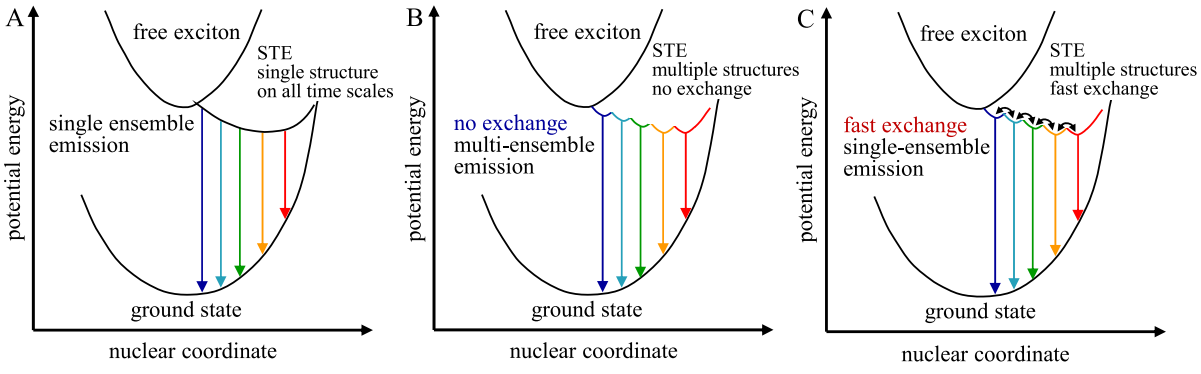

Figure 2. (A) A model in which there exists a single STE structure resulting in a single emissive ensemble. (B) A model in which there exist multiple STE structures with slow (or no) exchange between the structures, resulting in multiple emissive ensembles. (C) A model in which there exist multiple STE structures with fast exchange between the states, resulting in a single emissive ensemble. The time constant of this single ensemble emission is the average of all the time constants associated with different environments.

https://dx.doi.org/10.1021/jacs.0c05636
J. Am. Chem. Soc. 2020, 142, 16622−16631

Extrinsic self-trapping alone is not consistent with the results presented below. Extrinsic defects, such as vacancies, are essentially static on fast time scales. To account for the very broad continuous spectrum, there would have to be a very large number of such defects, or most excitations would emit as unperturbed STEs with extrinsic defect-perturbed STEs emitting at a number of other wavelengths with a range of lifetimes, and with low amplitude proportional to their concentration. A very high concentration of static defects is unlikely in the single crystals studied here. In addition, the time independence of the emission spectrum is also observed in the spin-coated film, which would be expected to have a much higher concentration of extrinsic defects that the single crystals.

We propose that fast structural fluctuations of the lattice, which give rise to transient local environments, influence the STEs. Ultrafast two-dimensional infrared spectroscopy studies on another layered lead perovskite have revealed structural fluctuations on a ~10 ps time scale.[26] For the almost instantaneous time scale of photon emission, the effectively static range of local environments (inhomogeneous broadening), plus the phonon-induced homogeneous broadening of each STE emission, results in the white-light spectrum. However, we propose that rapid structural fluctuations cause excitations to experience all environments faster than the emission decay time scale (see Figure 2C), resulting in identical emission dynamics at all wavelengths.

2. MATERIALS AND METHODS

All manipulations were performed in atmosphere unless otherwise noted. Solvents were of reagent grade or higher purity. All reagents were purchased from commercial vendors and used as received unless otherwise noted. The solvent dimethyl sulfoxide (DMSO) was dried and degassed using a JC Meyer solvent purification system.

Single crystals and thin films of (EDBE)$PbBr_4$ were synthesized through solution-state self-assembly. Single crystals were obtained by adding 1.0 mL of concentrated (9 M) aqueous hydrobromic acid to a mixture of 40−46 μL of 2,2′-(ethylenedioxy)bis(ethylamine) and 40−46 mg of $PbBr_2$ in a 4 mL shell vial. The solution was sonicated until all solids dissolved, and left covered and undisturbed at room temperature for a period of several days. The large, colorless, plate-like crystals that formed were carefully isolated and dried under reduced pressure. Due to the variability in crystal size, multiple crystallizations were set up to obtain large single crystals.

Precursor solutions for thin film deposition were prepared by first synthesizing a powder of (EDBE)$PbBr_4$ using an established synthesis.[12] Thin films were prepared following a modified version of a previously described preparation.[23] Fused silica substrates were prepared with a 15 min UV-ozone treatment immediately before being brought into a N_2-filled glovebox containing a spin coater. A 100 μL volume of the precursor solution of 0.25 M (EDBE)$PbBr_4$ in DMSO was deposited onto the substrate, which was spun for 45 s at 5000 rpm (4000 rpm/s acceleration) immediately before being annealed at 110 °C for 20 min. Crystals of (EDBE)$PbBr_4$ were placed between two 1 in. diameter fused silica windows separated by a 1 mm Teflon spacer. One quarter of a second 1 mm Teflon spacer was placed at the center of the fused silica such that the crystal could rest on it when the sample cell was held upright. The thin-film samples used two 1 in. fused silica windows, each coated with a thin film, placed in a lens mount such that the thin films faced each other separated by an O-ring.

Time-resolved photoluminescence population decay experiments were conducted utilizing time-correlated single photon counting (TCSPC). A Ti:sapphire oscillator producing approximately 100 fs pulses at an excitation wavelength of 730 nm was employed. This wavelength was frequency doubled in a barium borate crystal to 365 nm for excitation of the (EDBE)$PbBr_4$ perovskite. The bandwidth of the 365 nm excitation pulse was 5.8 nm, and the energy per pulse was 0.25 nJ. The laser repetition rate was lowered from 80 to 5 MHz by means of an acousto-optic modulator functioning as a single pulse selector. A computer-controlled half-wave plate was used to rotate the polarization of the excitation beam between vertical and horizontal. The photoluminescent emission was collected by a large lens focused with a second lens through a fixed polarizer set to horizontal polarization secured at the entrance slit of a monochromator. The sample was excited from the front surface in a near-normal geometry through a hole in the lens that collected the PL. Approximately one excitation event occurs per 5 million unit cells in the (EDBE)$PbBr_4$ crystal.

The instrument response was obtained by measuring the fluorescence lifetime of aqueous acidified malachite green in a 1 mm path length optical cell with an optical density matching that of the sample, under experimental conditions identical to those used in the sample measurements. Malachite green has an extremely short fluorescence lifetime, 5 ps, which is short compared to the instrument response.[28] The approximate thickness of the perovskite crystals used in the experiments is 1 mm. Measurement of malachite green's fluorescence emission with this system gives the instrument response, including the effects of the finite thickness of the sample cell at the emission wavelength observed in the experiments. The instrument response from the experiment can be seen in Figure S1 and had a standard deviation of 51 ps.

The PL was frequency resolved by the monochromator, and single photons were detected with a multi-channel plate (MCP) detector at wavelengths ranging from 380 to 700 nm in increments of 5 nm. In a single monochromator scan, each emission wavelength was collected for 15 s. The wavelength scan was repeated until it was determined that an acceptable signal-to-noise level had been reached. After one full scan of the wavelength range, the polarization was changed, alternating between vertical and horizontal polarizations in the lab frame. Once data at both polarizations were taken, the sample cell was translated using a computer-controlled motorized translation stage such that a new spot on the (EDBE)$PbBr_4$ crystal was excited. All data were taken with the same entrance slit width, and all other experimental conditions were identical so that the relative amplitudes at each emission wavelength were correct.

3. RESULTS AND DISCUSSION

In prior mechanistic studies on the (110) perovskite (*N*-MEDA)$PbBr_4$, transient absorption spectroscopy on thin films provided the first clear experimental evidence for the broadband emission originating from self-trapped excitons (STEs) that formed upon UV excitation. In that study, optical Kerr gating and time-correlated single photon counting (TCSPC) experiments on pressed pellets suggested that the broadband emission throughout the visible regime is the result of a variety of STEs where the states exhibited increasingly longer lifetimes as the emission wavelength became longer.[22] The experiments indicated a shift in the spectrum to lower frequency, as the higher frequency portions of the spectrum decayed prior to the lower frequency parts of the emission spectrum.

As discussed in the previous section, in this study a monochromator was scanned through the emission spectrum of a single crystal of (EDBE)$PbBr_4$, capturing the luminescent decays at a large number of wavelengths (200) over a very broad range of times. Before the time-resolved measurements are considered, we constructed a time-independent spectrum by integrating each luminescent decay along the time axis. This generates a spectrum that can be compared to a steady-state spectrum measured with a fluorometer. The time-independent spectra of 14 different crystal regions were examined using a relatively small laser spot size with full width at half-maximum of 550 μm, and it was determined that they were uniform, with

https://dx.doi.org/10.1021/jacs.0c05636
J. Am. Chem. Soc. 2020, 142, 16622−16631

the exception of one obtained on a location with a visible macroscopic imperfection. A photograph of the crystal and the time-independent spectra generated at each location are given in Figure S2.

Combining the data collected at all good crystal locations, the resulting population decays taken with vertically polarized excitation along the *ab* plane of the (EDBE)$PbBr_4$ crystal are displayed in Figure 3A. Note the significant differences in

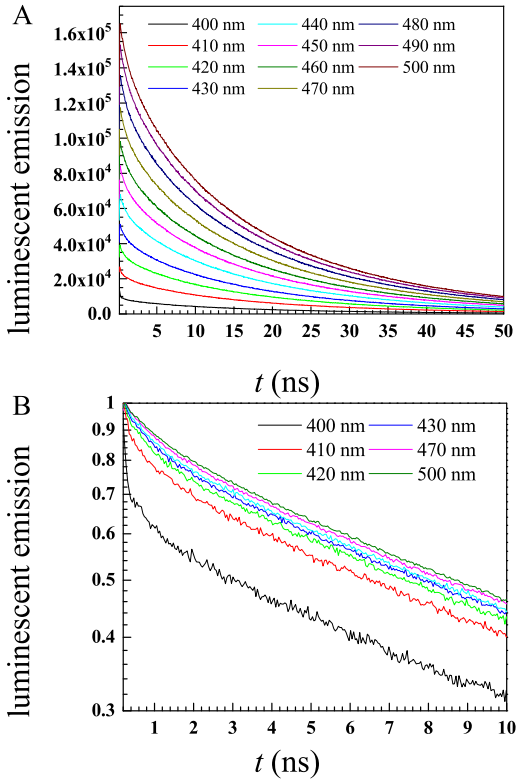

Figure 3. (A) Unnormalized luminescent emission at representative wavelengths. Each decay was collected for identical periods of time under the same experimental conditions. These decays at many wavelengths allow the time-dependent emission spectra to be constructed. (B) Early-time behavior of normalized luminescent emissions. The shorter wavelength emissions decay more rapidly than their longer wavelength counterparts, reproducing the behavior observed previously.[22] Only a subset of the traces from panel A were used for clarity.

emission amplitudes at each wavelength. Accurate relative amplitudes are necessary to construct the time-dependent spectra. Therefore, each decay was collected under identical conditions. Figure 3B shows the normalized decays on a semi-log plot highlighting the short time behavior. The emission on the bluer side of the spectrum decays more rapidly than on the redder side of the spectrum, as observed previously for (*N*-MEDA)$PbBr_4$ and (EDBE)$PbBr_4$ perovskites.[22,23] Looking only at the population decays at several wavelengths over a very limited time range, the observed behavior was attributed to a series of self-trapped excitons, each with its own lifetime.[22] But the time-dependent emission spectra presented below show that the luminescence consists of two distinct overlapping spectra with different photoluminescent emission properties. The vast majority of the emission has wavelength-independent time decays. Figure S3 highlights this wavelength-independent population decay after 1 ns by normalizing luminescent decays at a variety of emission wavelengths to their values at 15 ns. The time-dependent spectra of (EDBE)$PbBr_4$ are shown in Figure 4A. There is a very small

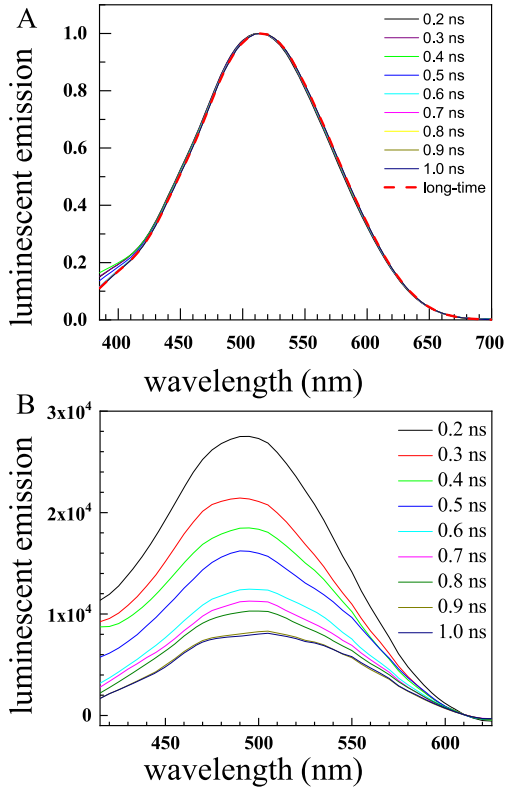

Figure 4. (A) Time-dependent emission spectra over the first nanosecond of the 100 ns experimental time window. A small change can be seen on the blue side of the spectrum, while the red side remains largely the same. (B) The spectra in panel A with a representative long-time spectrum (60 ns) subtracted from each. A peak centered at 490 nm, previously undifferentiated, can be observed decaying with a time constant of 0.6 ns.

change with time on the blue side of the spectrum, but it is difficult to characterize this feature further based solely on this plot. After ∼1 ns, the spectrum ceases to change other than decaying in amplitude (see below).

If a portion of the time-dependent emission spectrum changes with a different lifetime and a different emission line shape than the long-time spectrum, it cannot be considered part of the same ensemble. The change in the time-resolved emission spectrum as a function of time demonstrates the presence of at least two ensembles of emitters. However, because the emission spectrum is not changing for the vast majority of the experimental time window, the long-time spectrum reflects one of the ensembles of emitters. By scale subtracting the 60 ns long-time spectrum from each of the short-time spectra, the early-time spectral component responsible for the feature on the blue side of the total spectrum was isolated. The time-dependent spectra following subtraction are displayed in Figure 4B. Figure 4B shows that there is a small side peak centered at ∼490 nm, which is distinct from the spectrum observed on the single location that has a macroscopic imperfection (Figure S2A). The 490 nm side peak shown in Figure 4B is observed at all of the crystal locations as well as on other crystals. It decays rapidly with a time constant of 0.6 ns.

https://dx.doi.org/10.1021/jacs.0c05636
J. Am. Chem. Soc. 2020, 142, 16622−16631

When the broad emission from (*N*-MEDA)$PbBr_4$ was previously studied, decays at a few wavelengths were measured over a short time range, ~1.5 ns.[22] This early-time behavior was fit to a stretched exponential with a time constant varying between 0.45 and 0.65 ns (across the band from blue to red) and a single stretching constant of 0.65.[22] The results were interpreted as arising from a series of self-trapped states (self-trapped excitons interacting with lattice defects) with bluer emission wavelengths having faster decay rates than redder emission wavelengths.[22] The time constant of 0.6 ns obtained from the data in Figure 4B has the time scale of the dynamics observed in this previous study. However, the prior model is not consistent with the data presented in Figure 4 and below for single crystals of (EDBE)$PbBr_4$. If the broadband white-light emission arose from a series of statically perturbed self-trapped states, having different lifetimes and contributing to a part of the wavelength range encompassed by the broad emission, then there would be significant changes in the emission line shape as a function of time. A time-dependent line shape and different luminescent decay times are inconsistent with the data shown in Figure 4A. The blue side of the line would decay faster, causing the entire spectrum to shift to the red, as seen in pressed pellets of (*N*-MEDA)$PbBr_4$.[22] Except for the very blue edge, the spectra in Figure 4A are time-independent at short time to 1 ns as well as to very long times (100 ns).

Figure 5A shows the emission spectrum from 0.6 to 100 ns. By 2 ns, the 490 nm peak shown in Figure 4B, which has a small initial amplitude and a decay constant of 0.6 ns, makes a negligible contribution to the data. As can be seen in Figure 5A, the normalized spectra are essentially time-independent from 0.6 to 100 ns. There are 10 differently colored curves in this figure that are difficult to distinguish because they are identical within experimental error. The fact that the spectrum does not change shape from 0.6 to 100 ns is indicative of single ensemble emission (see below), and rules out a distribution of subensembles with different ns time scale decays with faster decays on the blue side of the emission band.

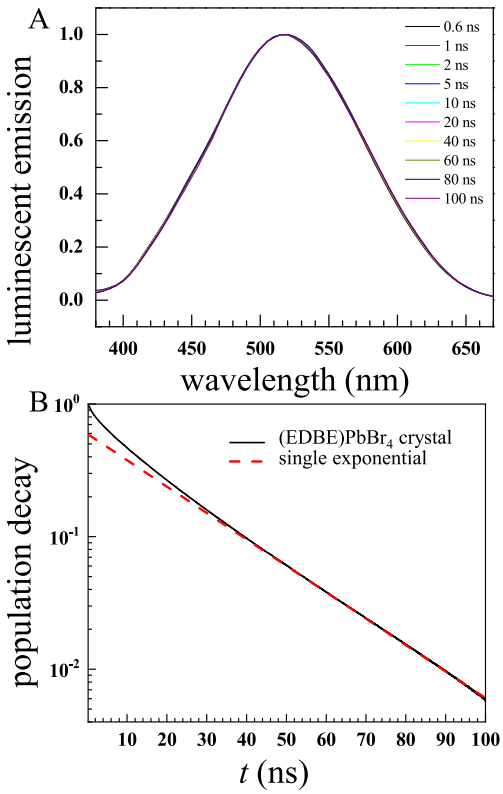

Figure 5. (A) Representative time-dependent emission spectra from 0.6 to 100 ns. The emission line shapes are identical throughout the experimental window after the first nanosecond. The spectra are so similar that it is difficult to discern the individual plots. (B) The tri-exponential population decay of (EDBE)$PbBr_4$. The red dashed line is the longest decay component, 21.8 ns.

Figure 5B shows a semi-log plot of the integrated population decay. The plot spans more than two decades in amplitude and approximately two decades in time. The spectral shapes are unchanging over a very long period of time, which demonstrates single ensemble emission. However, the decay from this single ensemble is definitely not a single exponential. The dashed red line is a single-exponential decay through the long-time portion of the data. The deviation from single-exponential decay behavior is clear at short times. Multiple types of fitting functions were tested to characterize the population decay of the white-light-emitting perovskite. Of these, two functions fit the data well by eye: a tri-exponential and the sum of a short-time stretched exponential and a long-time single exponential. Fits of both of the functions to the data are available in Figure S4, where the residuals are also shown. Although the residuals are somewhat worse for the sum of a short time stretched exponential and a long-time single exponential, the Akaike Information Criterion (AIC), a statistical test used to judge the efficacy of fitting functions, was employed to compare the quality of the two fitting functions.[29] AIC compares the quality of fits to a data set fit with the two fitting functions, taking into account differences in the number of adjustable parameters. The AIC test determined that the tri-exponential fit was significantly superior to that of a stretched exponential plus a single exponential. Therefore, it was concluded that the population decay of the main peak of (EDBE)$PbBr_4$ is a tri-exponential with time constants of 1.2, 8.5, and 21.8 ns. The dashed line in Figure 5B has an exponential decay constant of 21.8 ns. A prior study on (EDBE)$PbBr_4$ also fit the PL decay to three lifetimes. However, in contrast to the present study, these three lifetimes were attributed to three distinct excited-state subensembles emitting at different wavelengths. It should be noted that in this previous study, no time-resolved emission spectra were measured. The model was built by comparison of steady-state spectra and a small number of population decays.

Usually a non-exponential population decay would indicate multiple emitting ensembles, each with its own population lifetime. In this case, a tri-exponential would suggest three distinct ensembles. Could there be three ensembles with very different radiative rate constants that give rise to the three lifetimes, but still all have identical spectral shape? The radiative rate constant is determined by the absolute value squared of the transition dipole matrix element.[30] For the transition dipole matrix elements to differ, the excited-state wave function and/or the ground-state wave function must be different. In general, if the wave functions differ enough to make the transition dipole matrix elements sufficiently different to produce the observed large variation in decay constants, then the spectra will not be the same. Therefore, the tri-exponential decay does not arise from distinct ensembles with different radiative rate constants.

https://dx.doi.org/10.1021/jacs.0c05636
J. Am. Chem. Soc. 2020, 142, 16622−16631

If distinct radiative rate constants are not responsible for the tri-exponential decay, it must arise from differences in non-radiative relaxation mechanisms. Is it possible that there are three distinct ensembles with identical spectra and radiative rate constants but distinct non-radiative rate constants? Non-radiative relaxation occurs by the relaxation of the electronic excited state into an equienergetic collection of ground electronic state vibrations and phonons. A non-radiative rate constant is determined by the coupling matrix elements of the electronic excited state to lattice mechanical degrees of freedom and the density of states of ground-state vibrations and phonons at the excited-state energy. For there to be three distinct non-radiative rate constants arising from three distinct ensembles, one or more of the following must occur: the electronic excited states are coupled to different sets of lattice modes, the coupling constants differ, and/or the densities of states differ. The excited states are excitations of a large single crystal. For the lattice modes, the coupling to them, and the density of states to be sufficiently different to cause the large differences in decay, the environments in proximity to excitations should be very different and remain different on the time scale of the emission. Such large differences are highly unlikely and would give rise to distinct spectra for each of the three environments that would have to exist to generate the observed tri-exponential decay.

The existence of three distinct ensembles having identical spectra, but with either different radiative or non-radiative decay constants to produce a tri-exponential population decay, is not physically reasonable. We thus conclude that the tri-exponential emission is from a single ensemble of emitters following the rapid decay (0.6 ps) of the low-amplitude 490 nm band. However, this leaves the question of how a single emitting ensemble can give rise to a tri-exponential decay. Although there are no direct experimental data to answer this question, we consider two heuristic examples.

There could be an ensemble of defect sites in the lattice that have very fast radiationless relaxation. The defect sites do not appear in the emission spectrum because their luminescence quantum yield is extremely small since they undergo very fast, radiationless relaxation. If a defect site is adjacent to initial excitation, the exciton could hop onto the defect and decay without emission. The STE is far below the exciton band, and thermal promotion to the band is improbable. However, if the hypothetical defect site is similar to or lower in energy compared to the STE, then direct Förster-like transfer could occur without thermal promotion to the band. Förster transfer is short range, and the probability falls off as the sixth power of the separation of the donor (STE) and the acceptor (defect site). Transfer to a near neighbor could be responsible for the fastest decay component, 1.2 ns. If the defect site is farther away, say in the second shell around the initial excitation, the time to hop onto a defect would take longer and could give rise to the second decay constant, 8.5 ns. Given the short-range nature of Förster transfer, if a defect is even farther away, the STE cannot hop that far within its lifetime and decays with the slowest decay constant, 21.8 ns.

Another possibility involves the known mobility of defects such as halide vacancies in halide perovskites.[31] In this scenario, a mobile lattice defect moves onto the site of an immobile STE. The STE now on the defect site undergoes rapid, radiationless relaxation. If the defect mobility is low, then the fast decay component might occur if the defect is a near neighbor to the STE and the second slower decay component of the tri-exponential arises from a defect site in the second shell around the STE, which has to move farther to quench the STE. If the closest mobile defect to the STE is farther away, it does not encounter the STE during the ∼22 ns longest decay component of the luminescence. In both cases, the defects act as non-radiative sinks for the exciton. Therefore, the luminescence spectrum is not changed. The result is that the emitting excitons are a single ensemble with a single time-independent spectrum from 0.6 to 100 ns, but the decay is a tri-exponential. These heuristic examples are two potential explanations for the behavior observed in these white-light emitters. Other physical mechanisms may explain the observations demonstrated in this study, but any proposed mechanism must be able to reconcile the single time-independent emission spectrum and the tri-exponential population decay.

The single ensemble property of the fluorescence emission can be a result of the nature of the emitting states and the resulting line shape. Electronic spectra are, in general, a combination of homogeneous and inhomogeneous components. Homogeneous broadening can arise from strong coupling between the exciton and the lattice phonons, which also causes large lattice deformations in the excited state, leading to STEs. Inhomogeneous broadening is caused by excitations in different locales experiencing distinct environments that shift the center frequency of the homogeneously broadened line. These distinct environments that give rise to different optical frequencies would also likely result in multiple lifetimes because differences in local environments sufficient to result in substantial shifts in emission frequency would also change radiative and non-radiative rate constants. In addition, vibronic transitions from excited vibrations in the electronic excited state to vibrational levels of the ground state can cause broadening of the emission spectrum.

Figure 2A is a schematic of a single homogeneously broadened emitting state that includes vibronic transitions, but vibrational levels are not shown in the figure. Figure 2A represents a single electronic excited state. In this case, all STEs would be identical. Therefore, emission would be from a single ensemble and give rise to single ensemble luminescence decay, which is consistent with the observations as shown in Figure 5A. While this scenario cannot be ruled out, it is likely that homogeneous broadening through phonon coupling and vibronic transitions will not generate an emission spectrum that is broad enough to cover the entire visible spectrum. The visible spectrum is ∼10 000 cm^{-1} wide. Phonon broadening depends on the phonon bandwidths, which would be on the order of several hundred wavenumbers. The vibrational modes that will be strongly coupled to the electronic transition are the Pb−Br stretches with vibrational frequencies of ∼97 and 153 cm^{-1}.[12] There are many high- and low-frequency modes of the organic chains that bridge the layers, but these will not be coupled significantly to the electronic transition. kT at room temperature is ∼200 cm^{-1}, so several quantum levels of the low-frequency Pb−Br stretching modes will be populated in the electronic excited state. The emitting self-trapped excitons have a lattice configuration that is highly distorted from the initial ground-state structure, shifting the excited-state potential surface relative to that of the ground state. Thus, the vibronic transitions will be to ground-state vibrations with large quantum numbers. The emission from low quantum number vibrations of the excited state to high quantum number vibrations of the ground state will give rise to poor

https://dx.doi.org/10.1021/jacs.0c05636
J. Am. Chem. Soc. 2020, 142, 16622−16631

Franck−Condon factors but will potentially result in a long progression of vibronic states. Each of these vibronic emissions will be broad and overlapping because of the phonon homogeneous broadening. As the ground states have high quantum numbers, anharmonicity will make their energy spacings significantly less than the fundamental frequencies. Then a progression of 10−15 transitions could produce an emission width of 1000 cm^{-1}, even possibly 2000 cm^{-1}, but still not enough to span the entire visible spectrum.

For comparison consider the emission spectrum of the dye molecule rhodamine 6G (R6G) in ethanol. Instead of phonons, the solvent has a continuum of intermolecular modes. Because of hydrogen bonding, the continuum is broad, on the order of 600 cm^{-1}. R6G, which is a multi-ring system, has low frequency, intermediate frequency, and high-frequency modes coupled to the electronic transition. It has a broad emission. The width from 10% intensity on the blue to 10% intensity on the red sides of the fluorescence line is 525−625 nm, which is ∼3000 cm^{-1}. For the STE emission to occur as a homogeneous line with vibronic transitions that spans the visible spectrum, it needs to be more than 3 times broader than the R6G emission. While this is possible, it seems likely that the observed width of the STE emission has additional inhomogeneous broadening.

Figure 2B,C shows schematics of the STE excited state with inhomogeneous broadening. Again, vibrational levels that would give rise to vibronic transitions in the excited and ground states are not shown. The wells indicate different local structures that would shift the STE energy. In contrast to the schematic of inhomogeneous broadening shown in Figure 2B,C as a few distinct potential wells, in a real system, there would be a virtual continuum of such wells. In Figure 2B, the local structures that give rise to inhomogeneous broadening are static, at least on a time scale that is long compared to the emission decay. Differences in local environment sufficient to cause substantial changes in the electronic wavefunctions responsible for large spectral shifts, would also be expected to change the radiative and non-radiative decay times, and therefore the overall emission decay time. Say for example that environments that blue shift excitations also result in shorter lifetimes, while environments that red shift excitations produce longer lifetimes. Then the spectrum would have a time-dependent shape. On average, excitations on the blue side of the line will decay sooner, resulting in a red shift of the emission and narrowing of the spectrum with time. Such shifting and narrowing does not occur for the perovskite crystal studied here (see Figure 5A).

In contrast to Figure 2B, Figure 2C illustrates the case of inhomogeneous broadening in which the local environments interconvert one to another. This interconversion results in any excitations sampling all possible local structures on a time scale that is fast compared to the emission decay time. On a very short time scale, various excitations in the heterogeneous lattice will have different properties. However, structural fluctuations will cause the frequencies of the excitations to evolve in time, which is called spectral diffusion. (The existence of inhomogeneous broadening and the rate of spectral diffusion can be measured with ultrafast 2D electronic spectroscopy.[32,33]) For an emission time scale that is long compared to the spectral diffusion, an excitation will have sampled all possible frequencies (Figure 2C). However, at the instant of fluorescence emission, an excitation will have a particular frequency within the inhomogeneously broadened line. Therefore, the emission is very broad reflecting the combined broadening effects of homogeneous broadening, inhomogeneous broadening, and a progression of vibronic transitions.

Previously, 2D IR spectroscopy on the layered Pb-I perovskite $(CH_3NH_3)_2PbI_2(SCN)_2$ showed ultrafast dynamics that occurred in the inorganic components of the lattice with a vibrational spectral diffusion time constant of 4.1 ps.[26] It is important to note the spectral diffusion was measured for the ground electronic state of the perovskite. However, these structural fluctuations, measured via their effect on a vibration, should influence the electronic excited state as well as the ground state. It is likely that the (EDBE)$PbBr_4$ lattice will also have structural fluctuations that give rise to excited electronic state spectral diffusion on a time scale that is very fast compared to the emission, that is <1 ns. Other studies have also revealed fast dynamics in the inorganic sublattice of halide perovskites.[3,5]

If fluctuating lattice structures that give rise to inhomogeneous broadening undergo structural interconversion (spectral diffusion) on fast time scales compared to the nanosecond time scales of the emission, then there will be a common time-dependent fluorescence decay across the entire fluorescence band, as seen in (EDBE)$PbBr_4$. A given excitation will undergo emission, an essentially instantaneous process, at a particular frequency. However, prior to that, it will have sampled all possible environments and lifetimes. By spending a short amount of time with every environment and associated lifetime, the decays at all frequencies will be identical, as observed, and is the average decay (Figure 2C).

The time-independent emission line shape for times greater than ∼600 ps (Figure 5A) and the single decay curve across the entire fluorescence spectrum observed here are in contrast to the observations for pressed pellets of (*N*-MEDA)$PbBr_4$.[22] It should be noted that in the present work, crystals and thin films of (EDBE)$PbBr_4$ were studied as opposed to pressed pellets. For (*N*-MEDA)$PbBr_4$, the different lifetimes for different emission wavelengths were associated with distinct structures that do not rapidly interconvert.[22] Indeed, the observed emission redshift with time was consistent with this multi-ensemble model. In contrast, the model presented here for (EDBE)$PbBr_4$ single crystals and thin films (see below) is of a homogeneously and inhomogeneously broadened emission line with spectral diffusion that is much faster than the fluorescence decay. This picture is of a single emission ensemble in which all emitting sites are time averaged to be equivalent although there is rapidly fluctuating structural disorder.

The effects of sample morphology were also studied, comparing the PL of (EDBE)$PbBr_4$ large single crystals discussed above to that of thin films. While many qualities are the same, such as the presence of the 490 nm side peak, which quickly decays (0.6 ns), a striking difference was observed in the longer time scale population decay shown in Figure 6. The thin films have a bi-exponential fluorescence decay with a much lower amplitude weighted average luminescent time constant, τ_{pl}, than was observed for the crystals (see Table 1).

While the film's two time constants are similar to the two faster time constants of the single crystal, the longest single-crystal time constant is absent for the films. Similar to the crystals, the films are oriented with the inorganic sheets stacking along the thickness of the film (the *b* axis), but the films' *ac* planes are randomly oriented about the *b* axis. The

https://dx.doi.org/10.1021/jacs.0c05636
J. Am. Chem. Soc. 2020, 142, 16622−16631

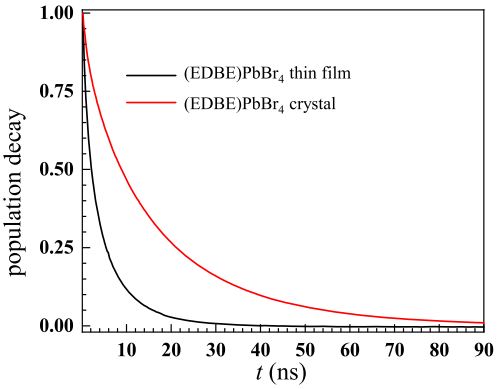

Figure 6. Comparison of the population decays of (EDBE)$PbBr_4$ from a spin-coated thin film and a large single crystal. The thin-film emission decays much more rapidly than the single crystal emission. The thin-film decay is bi-exponential, while the single crystal decay is tri-exponential. See Table 1 for time constants and amplitudes.

major difference between the single crystals and the films is the crystal size. In the thin films (1 in. in diameter with a thickness of ~80 nm), the area of the crystallites in the *ac* plane are on the order of 100 nm^2 while the crystal is macroscopic (~1 cm^2) as shown in Figure S2A. The *a* and *c* lattice dimensions of (EDBE)$PbBr_4$ yield a footprint of 0.56 nm^2. Thus a single grain in the film contains approximately 180 unit cells at the surface. Therefore, a significant fraction of the unit cells is close to the surface of the grains, and near grain boundaries where there can be more defects. In addition, the films are spin coated, which means the crystals grow in seconds in contrast to the large single crystals, which are formed over days. Thus, far more defects are expected in the film crystallites than in the large single crystals. As discussed above, to account for a single ensemble luminescence that decays as a tri-exponential, it was suggested that defects may facilitate non-radiative decay. If the defects in the films are far more numerous than in the large single crystals, all the STEs might be quenched by defects and decay non-radiatively. The result could be the elimination of the slow, 21.8 ns decay component observed in the large crystals, reducing the film decay to a bi-exponential.

The photoluminescent quantum efficiencies (PLQEs) of white-light-emitting perovskites are of particular interest due to their potential use as phosphors for artificial illumination. Thin films are the morphology that may be more useful for this application. While the PLQEs of these perovskites as crystals have been rigorously assessed,[11] thin film PLQEs are not as well studied. While there exist PLQE studies of drop cast microcrystalline films,[34] the domain size of these films is on the micrometer scale rather than the nanometer scale one would typically associate with thin films. If the faster population decay of the thin films (see Figure 6 and Table 1) is in fact caused by enhanced radiationless relaxation, then the film PLQE would be smaller. It will be important to study the dynamics and PLQEs of thin films for different methods of preparation.

4. CONCLUDING REMARKS

In this study, the time-dependent fluorescence emission of the white-light-emitting 2D perovskite (EDBE)$PbBr_4$ was investigated. The study was conducted on large single crystals and spin-coated thin films. Luminescent decays were collected across the perovskite's very broad bandwidth emission window. By measuring each decay for the same amount of time and under identical experimental conditions, it was possible to construct the time-dependent emission spectrum of the chromophore.

The time-dependent emission spectrum had a low-amplitude feature on the blue side of the main emission band with a short lifetime (600 ps). After the decay of this small, short-lived feature, the emission line shape remained constant for the duration of the experimental window, ~100 ns (Figure 5A). This time-independent spectrum demonstrates single ensemble emission. Intriguingly, despite being produced by a single ensemble, the population decay of the main spectral band in single crystals of (EDBE)$PbBr_4$ was non-exponential. The decay was tri-exponential, with time constants of 1.20, 8.48, and 21.75 ns.

White-light emission from 2D perovskites has been previously assigned to self-trapping of excitons in a deformable lattice, with the temperature dependence of the PL line width suggesting both intrinsic (self-trapping leading to a single distorted excited state) and extrinsic self-trapping (where permanent lattice defects affect the distorted excited states to give a distribution of such states).[11,12] Prior work studying the PL onset and decay times pointed to a wavelength dependence of the emission, with the lower-energy portion of the white emission showing slower onset and decay rates compared to the higher-energy portion of the spectrum.[22] The mechanism invoked a number of subensembles of self-trapped excitons. Each subensemble had a different emission wavelength, and their combination gave rise to the broadband white emission. These proposed subensembles also had different lifetimes, with the higher energy self-trapped excitons having shorter lifetimes. This model was used to explain the observation (which occurred over a short time period, ~1.5 ns, and at a small number of wavelengths) that the spectrum of a powder sample of (*N*-MEDA)$PbBr_4$ appeared to shift to the red as time progressed. As shown in Figure 5A, the spectrum of a single crystal of (EDBE)$PbBr_4$ does not display a time-dependent spectral shift. The apparent shift at short time is caused the decay of a relatively low amplitude band that is to the blue of the main band and relaxes in 600 ps (see Figure 4B). The data presented here eliminates a wavelength dependence to the principal emission band, showing that the emission from ca. 400 to 700 nm in (EDBE)$PbBr_4$ originates from a time-averaged single ensemble of excited states.

We propose that the observed broad single ensemble emission in this class of perovskites is caused by a combination of homogeneous and inhomogeneous broadening with spectral diffusion that is fast relative to the luminescent decay of the perovskite. On a very short time scale there is inhomogeneity,

Table 1. Population Decay Time Constants and Normalized Amplitudes of (EDBE)$PbBr_4$

sample	A_1	τ_1 (ns)	A_2	τ_2 (ns)	A_3	τ_3 (ns)	τ_{pl} (ns)[a]
crystal	0.13	1.20 ± 0.01	0.29	8.48 ± 0.02	0.58	21.75 ± 0.01	15.20 ± 0.01
thin film	0.49	1.46 ± 0.03	0.51	6.70 ± 0.04	N/A	N/A	4.11 ± 0.04

[a] τ_{pl} is the amplitude weighted average decay constant: $\tau_{pl} = \sum_i A_i \tau_i$.

https://dx.doi.org/10.1021/jacs.0c05636
J. Am. Chem. Soc. 2020, 142, 16622−16631

i.e., a distribution of self-trapped excitonic states that produce a range of excited-state energies, and in principle could have distinct lifetimes. However, the nature of these environments fluctuates so rapidly that any excitation experiences all local structures on a much faster time scale than that of fluorescence emission and, therefore, emits with the average lifetime. We further suggest that the non-exponential lifetime may be caused by the presence of defects in the lattice. When an exciton encounters a defect, either by motion of the defect or Förster-like excitation transfer, it undergoes very fast radiationless relaxation, returning to the ground state with negligible fluorescence emission. Such processes would not affect the emission line shape, but they would give rise to fluorescence decay that is not single exponential.

There are many additional spectroscopic studies that would increase our understanding of broadband white-light-emitting perovskites. The effects of temperature on the population decays of both large crystals and thin films may help in understanding the source of the multi-exponential decays. In thin films, comparing luminescent decays for crystallites of various sizes could help explain the origin of the bi-exponential decays observed for the films vs the tri-exponential decays observed for the large single crystals. It will be important to determine if there exists a correlation between the PLQE of a material and its luminescent lifetime. 2D electronic spectroscopy could be used investigate the model proposed here, i.e., spectral diffusion throughout the inhomogeneously broadened excited-state spectrum that is fast compared to the luminescence decay gives rise to the single ensemble broad emission.

■ ASSOCIATED CONTENT

Supporting Information

The Supporting Information is available free of charge at https://pubs.acs.org/doi/10.1021/jacs.0c05636.

Time-resolved emission spectra methodology; Figure S1, instrument response; polarization considerations; macroscopic defects in (EDBE)$PbBr_4$, including Figure S2; Figure S3, population decays normalized at 15 ns; and Figure S4, fits to integrated population decays (PDF)

■ AUTHOR INFORMATION

Corresponding Authors

Hemamala I. Karunadasa − *Department of Chemistry, Stanford University, Stanford, California 94305, United States; Stanford Institute for Materials and Energy Sciences, SLAC National Accelerator Laboratory, Menlo Park, California 94025, United States;* orcid.org/0000-0003-4949-8068; Email: hemamala@stanford.edu

Michael D. Fayer − *Department of Chemistry, Stanford University, Stanford, California 94305, United States;* orcid.org/0000-0002-0021-1815; Email: fayer@stanford.edu

Authors

Joseph E. Thomaz − *Department of Chemistry, Stanford University, Stanford, California 94305, United States*

Kurt P. Lindquist − *Department of Chemistry, Stanford University, Stanford, California 94305, United States*

Complete contact information is available at: https://pubs.acs.org/10.1021/jacs.0c05636

Notes

The authors declare no competing financial interest.

■ ACKNOWLEDGMENTS

This work was supported by the Air Force Office of Scientific Research grant number FA9550-16-1-0104 (J.E.T. and M.D.F.). J.E.T. also thanks the NSF for partial support through a graduate research fellowship. K.P.L. thanks the Center for Molecular Analysis and Design for a graduate research fellowship. Work by K.P.L. and H.I.K. was supported by the National Science Foundation (DMR-1904443).

■ REFERENCES

(1) Stranks, S. D.; Snaith, H. J. Metal-Halide Perovskites for Photovoltaic and Light-Emitting Devices. *Nat. Nanotechnol.* **2015**, *10*, 391.

(2) Bakulin, A. A.; Selig, O.; Bakker, H. J.; Rezus, Y. L.; Müller, C.; Glaser, T.; Lovrincic, R.; Sun, Z.; Chen, Z.; Walsh, A.; et al. Real-Time Observation of Organic Cation Reorientation in Methylammonium Lead Iodide Perovskites. *J. Phys. Chem. Lett.* **2015**, *6*, 3663.

(3) Wu, X.; Tan, L. Z.; Shen, X.; Hu, T.; Miyata, K.; Trinh, M. T.; Li, R.; Coffee, R.; Liu, S.; Egger, D. A.; et al. Light-Induced Picosecond Rotational Disordering of the Inorganic Sublattice in Hybrid Perovskites. *Sci. Adv.* **2017**, *3*, e1602388.

(4) Poglitsch, A.; Weber, D. Dynamic Disorder in Methylammoniumtrihalogenoplumbates (II) Observed by Millimeter-Wave Spectroscopy. *J. Chem. Phys.* **1987**, *87*, 6373.

(5) Yaffe, O.; Guo, Y.; Tan, L. Z.; Egger, D. A.; Hull, T.; Stoumpos, C. C.; Zheng, F.; Heinz, T. F.; Kronik, L.; Kanatzidis, M. G.; et al. Local Polar Fluctuations in Lead Halide Perovskite Crystals. *Phys. Rev. Lett.* **2017**, *118*, 136001.

(6) Mitzi, D. B. Synthesis, Structure, and Properties of Organic-Inorganic Perovskites and Related Materials. *Prog. Inorg. Chem.* **2007**, 1.

(7) Smith, M. D.; Connor, B. A.; Karunadasa, H. I. Tuning the Luminescence of Layered Halide Perovskites. *Chem. Rev.* **2019**, *119*, 3104.

(8) Kitazawa, N. Excitons in Two-Dimensional Layered Perovskite Compounds:(C6H5C2H4NH3) 2Pb (Br, I) 4 and (C6H5C2H4NH3) 2Pb (Cl, Br) 4. *Mater. Sci. Eng., B* **1997**, *49*, 233.

(9) Dohner, E. R.; Hoke, E. T.; Karunadasa, H. I. Self-Assembly of Broadband White-Light Emitters. *J. Am. Chem. Soc.* **2014**, *136*, 1718.

(10) Muljarov, E.; Tikhodeev, S.; Gippius, N.; Ishihara, T. Excitons in Self-Organized Semiconductor/Insulator Superlattices: Pbi-Based Perovskite Compounds. *Phys. Rev. B: Condens. Matter Mater. Phys.* **1995**, *51*, 14370.

(11) Smith, M.; Karunadasa, H. White-Light Emission from Layered Halide Perovskites. *Acc. Chem. Res.* **2018**, *51*, 619.

(12) Dohner, E. R.; Jaffe, A.; Bradshaw, L. R.; Karunadasa, H. I. Intrinsic White-Light Emission from Layered Hybrid Perovskites. *J. Am. Chem. Soc.* **2014**, *136*, 13154.

(13) Smith, M. D.; Jaffe, A.; Dohner, E. R.; Lindenberg, A. M.; Karunadasa, H. I. Structural Origins of Broadband Emission from Layered Pb−Br Hybrid Perovskites. *Chem. Sci.* **2017**, *8*, 4497.

(14) Mao, L.; Wu, Y.; Stoumpos, C. C.; Wasielewski, M. R.; Kanatzidis, M. G. White-Light Emission and Structural Distortion in New Corrugated Two-Dimensional Lead Bromide Perovskites. *J. Am. Chem. Soc.* **2017**, *139*, 5210.

(15) Thirumal, K.; Chong, W. K.; Xie, W.; Ganguly, R.; Muduli, S. K.; Sherburne, M.; Asta, M.; Mhaisalkar, S.; Sum, T. C.; Soo, H. S.; Mathews, N. Morphology-Independent Stable White-Light Emission from Self-Assembled Two-Dimensional Perovskites Driven by Strong Exciton−Phonon Coupling to the Organic Framework. *Chem. Mater.* **2017**, *29*, 3947.

(16) Mao, L.; Wu, Y.; Stoumpos, C. C.; Traore, B.; Katan, C.; Even, J.; Wasielewski, M. R.; Kanatzidis, M. G. Tunable White-Light Emission in Single-Cation-Templated Three-Layered 2D Perovskites

(CH3CH2NH3) 4Pb3Br10−X Cl X. *J. Am. Chem. Soc.* **2017**, *139*, 11956.
(17) Neogi, I.; Bruno, A.; Bahulayan, D.; Goh, T. W.; Ghosh, B.; Ganguly, R.; Cortecchia, D.; Sum, T. C.; Soci, C.; Mathews, N.; Mhaisalkar, S. G. Broadband-Emitting 2 D Hybrid Organic−Inorganic Perovskite Based on Cyclohexane-Bis (Methylamonium) Cation. *ChemSusChem* **2017**, *10*, 3765.
(18) Yangui, A.; Garrot, D.; Lauret, J.-S.; Lusson, A.; Bouchez, G.; Deleporte, E.; Pillet, S.; Bendeif, E.-E.; Castro, M.; Triki, S. Optical Investigation of Broadband White-Light Emission in Self-Assembled Organic−Inorganic Perovskite (C6H11NH3) 2PbBr4. *J. Phys. Chem. C* **2015**, *119*, 23638.
(19) Guo, X.; Houser, K. W. A Review of Colour Rendering Indices and Their Application to Commercial Light Sources. *Lighting Res. Technol.* **2004**, *36*, 183.
(20) Narendran, N.; Deng, L. *Solid State Lighting II*; International Society for Optics and Photonics, 2002; Vol. *4776*, p 61.
(21) Pimputkar, S.; Speck, J. S.; DenBaars, S. P.; Nakamura, S. Prospects for Led Lighting. *Nat. Photonics* **2009**, *3*, 180.
(22) Hu, T.; Smith, M. D.; Dohner, E. R.; Sher, M.-J.; Wu, X.; Trinh, M. T.; Fisher, A.; Corbett, J.; Zhu, X.-Y.; Karunadasa, H. I.; Lindenberg, A. M. Mechanism for Broadband White-Light Emission from Two-Dimensional (110) Hybrid Perovskites. *J. Phys. Chem. Lett.* **2016**, *7*, 2258.
(23) Cortecchia, D.; Yin, J.; Bruno, A.; Lo, S.-Z. A.; Gurzadyan, G. G.; Mhaisalkar, S.; Brédas, J.-L.; Soci, C. Polaron Self-Localization in White-Light Emitting Hybrid Perovskites. *J. Mater. Chem. C* **2017**, *5*, 2771.
(24) Arora, N.; Dar, M. I.; Hinderhofer, A.; Pellet, N.; Schreiber, F.; Zakeeruddin, S. M.; Grätzel, M. Perovskite Solar Cells with Cuscn Hole Extraction Layers Yield Stabilized Efficiencies Greater Than 20%. *Science* **2017**, *358*, 768.
(25) Cha, W.; Kim, H.-J.; Lee, S.; Kim, J. Size-Controllable and Stable Organometallic Halide Perovskite Quantum Dots/Polymer Films. *J. Mater. Chem. C* **2017**, *5*, 6667.
(26) Nishida, J.; Breen, J. P.; Lindquist, K. P.; Umeyama, D.; Karunadasa, H. I.; Fayer, M. D. Dynamically Disordered Lattice in a Layered Pb-I-SCN Perovskite Thin Film Probed by Two-Dimensional Infrared Spectroscopy. *J. Am. Chem. Soc.* **2018**, *140*, 9882.
(27) Byun, J.; Cho, H.; Wolf, C.; Jang, M.; Sadhanala, A.; Friend, R. H.; Yang, H.; Lee, T. W. Efficient Visible Quasi-2D Perovskite Light-Emitting Diodes. *Adv. Mater.* **2016**, *28*, 7515.
(28) Wirth, P.; Schneider, S.; Dörr, F. S1-Lifetimes of Triphenylmethane and Indigo Dyes Determined by the Two-Photon-Fluorescence Technique. *Opt. Commun.* **1977**, *20*, 155.
(29) Bozdogan, H. Model Selection and Akaike's Information Criterion (AIC): The General Theory and Its Analytical Extensions. *Psychometrika* **1987**, *52*, 345.
(30) Fayer, M. D. *Elements of Quantum Mechanics*; Oxford University Press on Demand, 2001.
(31) Senocrate, A.; Maier, J. Solid-State Ionics of Hybrid Halide Perovskites. *J. Am. Chem. Soc.* **2019**, *141*, 8382.
(32) Yan, C.; Yuan, R.; Nishida, J.; Fayer, M. D. Structural Influences on the Fast Dynamics of Alkylsiloxane Monolayers on SiO2 Surfaces Measured with 2D IR Spectroscopy. *J. Phys. Chem. C* **2015**, *119*, 16811.
(33) Read, E. L.; Engel, G. S.; Calhoun, T. R.; Mančal, T.; Ahn, T. K.; Blankenship, R. E.; Fleming, G. R. Cross-Peak-Specific Two-Dimensional Electronic Spectroscopy. *Proc. Natl. Acad. Sci. U. S. A.* **2007**, *104*, 14203.
(34) Yuan, Z.; Zhou, C.; Messier, J.; Tian, Y.; Shu, Y.; Wang, J.; Xin, Y.; Ma, B. A Microscale Perovskite as Single Component Broadband Phosphor for Downconversion White-Light-Emitting Devices. *Adv. Opt. Mater.* **2016**, *4*, 2009.

https://dx.doi.org/10.1021/jacs.0c05636
J. Am. Chem. Soc. 2020, 142, 16622−16631